Stereoscopic observations of the Crab Nebula with the HEGRA system of imaging air Čerenkov telescopes

A. Konopelko, G. Pühlhofer,

for the HEGRA Collaboration

Max-Planck-Institut für Kernphysik, Heidelberg D-69029, Postfach 10 39 80, Germany

Abstract. The HEGRA system of 5 imaging air Čerenkov telescopes was used for the extensive observations of the Crab Nebula. The observations have been extended to the zenith angles as large as 65 degree. Here we present the results of the data analysis in particular for the data taken at large zenith angles. LZA observations significantly improve the statistics for the γ-rays of energy above 5 TeV. Resulting spectrum of the Crab Nebula does not show apparent curvature in this energy range and may be fitted by pure power law in the energy range from 500 GeV to 20 TeV.

INTRODUCTION

The sensitivity of imaging atmospheric Čerenkov telescopes (IACTs) in TeV γ-ray observations reaches its maximum at small zenith angles ($\leq$30 degree) which permits the minimum attainable energy threshold of an instrument and detection of high quality two-dimensional angular images of Čerenkov light from air showers. However, for a specific telescope site a number of γ-ray sources, or source candidates, can only be observed at much larger zenith angles (LZAs). Extension of observations to LZAs might substantially widen the observational time window. Apparently that is very important for multi-wavelength campaigns involving ground-based and satellite-born instruments in simultaneous observations of variable γ-ray sources, e.g. BL Lac objects. In addition, observations at LZAs favor the detection of the high energy γ-rays (E > 10 TeV) which, at present, can be registered only using the ground-based Čerenkov technique.

We present here the results respecting the sensitivity and measurements of the energy spectra in stereoscopic observations of the Crab Nebula at LZAs ($\simeq$65 degree) with the HEGRA system of IACTs.

The HEGRA IACT system was primarily designed for detailed spectral measurements of TeV γ-rays, utilizing the advantages of the stereoscopic observations.

Stereo imaging allows (i) direct measurement of shower impact parameter with accuracy better than 10 m; (ii) good energy resolution of 18%; (iii) extended abilities for systematic studies using several images for an individual shower. The detailed systematic studies for the spectrum evaluation technique for observations at small zenith angles (<30 degree) have been recently completed using Mrk 501 1997 data [1]. Here we present the Crab Nebula data taken with the the HEGRA system of IACTs in two 97/98 and 98/99 observation campaigns, in particular data taken at LZAs ($\simeq 60°$). The LZA data were analyzed using new analysis technique for the stereoscopic observations [2].

OBSERVATIONS

The Crab Nebula was extensively observed with the HEGRA IACT system in two observational seasons from Sep'97 to Mar'98 and from Oct'98 to Apr'99. The HEGRA system of IACTs is located at La Palma, Canary Islands. Since Oct'98 HEGRA collaboration operates 5 telescopes. Each of the telescopes consists of a 8.5 m^2 reflector focusing onto a photo multiplier tube camera. The number of photo multipliers in the camera was 271, which were arranged in a hexagonal matrix covering a field of view with a radius of $2.°3$. Any telescope camera was triggered when the signal in two neighbours of the 271 photo multiplier tubes exceeded a threshold of 8 photoelectrons, and the system readout started when at least two telescopes were triggered by Čerenkov light from air shower. The detection rate was 12.6 Hz near the zenith in Dec'97 and dropped down to about 10 Hz in Dec'99 for the 4 telescope system due to aging of the PMTs and reduced mirror reflectivity.

The Crab was observed in a wobble mode; i.e., the telescopes were pointed in Declination $\pm 0.5°$ aside from the nominal Crab position (a sign of angular shift was altered from one run of 20 min to another). This is useful for continuous monitoring of the cosmic ray background taking the OFF-source region being symmetric about the camera center, and 1° apart relative to the ON-source region. Observations of the Crab at zenith angles up to 50 degree were made in a period from Sep'97 to Mar'98, for a total of 82.5 hrs. During the last observational period in addition to the observations at zenith angles less than 50° for 76.1 hrs we have carried out the observations at LZAs ($50° < \theta < 65°$) for a total of 24 hrs in order to study the performance of the telescope system at LZA and to extend measurements of the Crab Nebula energy spectrum beyond 10 TeV.

The collection areas, as a function of energy and zenith angle, for γ-ray showers has been inferred from Monte Carlo simulations as described in [3]. The energy threshold of the telescope system, defined as the energy at which the γ-ray detection rate reaches its maximum for the differential spectrum $\mathrm{dN_\gamma/dE \sim E^{-2.5}}$, is ~ 0.5 TeV at small zenith angles, and increases up to ~ 5 TeV at 60° zenith angle. The simulations have been tuned for the different system configurations of 3,4 and 5 telescopes. The energy spectra derived for the different configurations have been gathered in the overall spectrum.

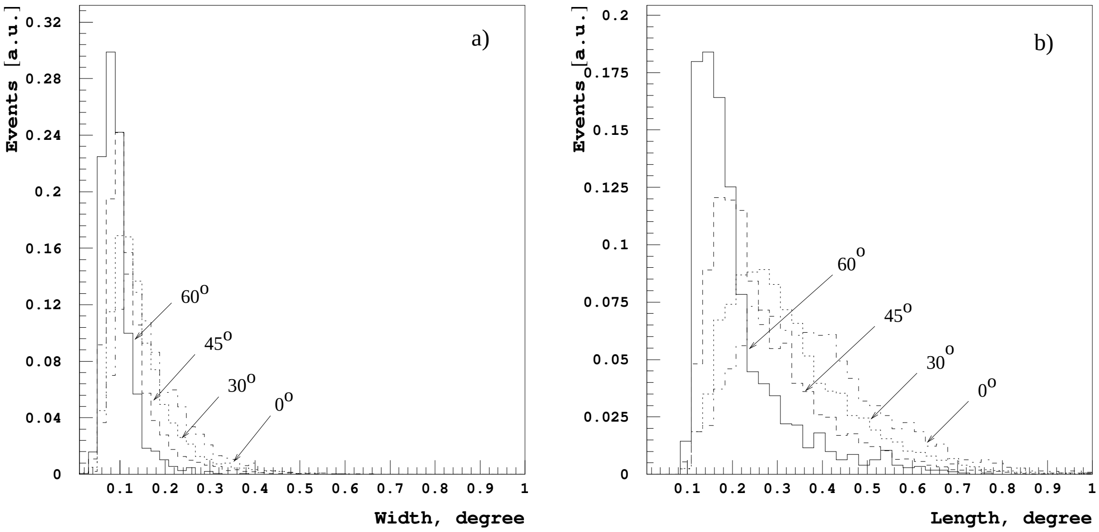

FIGURE 1. Distributions of image shape parameters for a $3 \div 5$ TeV γ-ray showers simulated at different zenith angles of $0°, 30°, 45°, 60°$.

ANALYSIS

The *stereoscopic imaging* analysis of the data is based on the geometrical reconstruction of shower arrival direction and shower core position in observation plane, as well as on the joint parameterization of a shape of the Čerenkov light images. The simultaneous registration of several ($\geq$2) Čerenkov light images from air shower provided an angular resolution of $\sim 0.°1$ for γ-ray showers. For each individual shower stereoscopic observations permit the determination of the position of the shower axis in the observation plane. We selected only air showers within a certain impact distance R_0 from the center of the telescope system. The limiting upper radius for zenith angles less than 50 degrees was 200 m and a significantly larger radius of 400 m was used for LZAs. For the data taken at zenith angles up to 50° we applied an orientation cut $\theta^2 < 0.05\,[\mathrm{deg}^2]$, where θ^2 is the squared angular distance of the reconstructed source position from the true source position. In addition we analyzed the data by *mean scaled Width* parameter, $< \tilde{w} >$. We used relatively loose cut, $< \tilde{w} >< 1.2$.

For the air showers at LZAs, the height of shower maximum is far above the observation level, and the geometrical distance from the shower maximum to the observer is correspondingly very large. That basicly determines the topology of Čerenkov light images from such showers. In Figure 1 the distributions of the image shape parameters are shown for the different LZAs: $0°, 30°, 45°, 60°$. The calculations have been done for the primary $3 \div 5$ TeV γ-rays. One can see that both the transverse (Width) and longitudinal (Length) angular size of Čerenkov light images become smaller at LZAs. Air showers of the same primary energy generate less density of the Čerenkov light at the observation level resulting, on

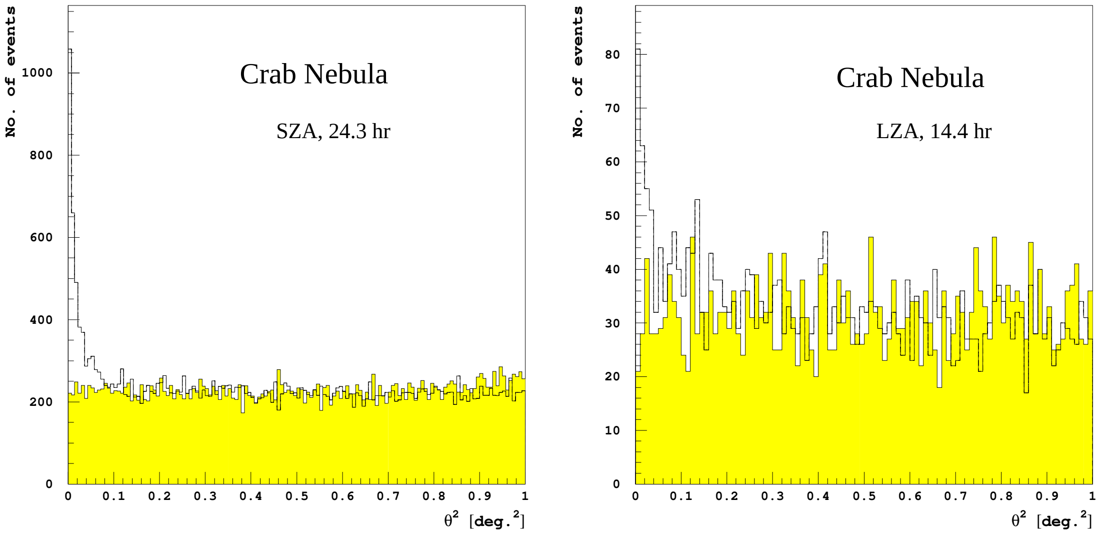

FIGURE 2. The event distribution as a function of θ^2 parameter for the ON and OFF (shaded histogram) regions for Crab Nebula observations at small ($\theta \leq 25°$) and LZAs ($55° \leq theta \leq 65°$).

average, in smaller number of Čerenkov photons in image. Calculations show that the images from LZA showers have almost circular shape and the image ellipticity, $1 - Width/Length$, noticeably decreases. The orientation of such images can be determined with large errors. That results in large uncertainties in the shower reconstruction, i.e., determination of the shower arrival direction, impact parameter, shower energy etc, and worse cosmic ray rejection. Thus the angular cut, $\theta^2 < 0.1\,[\mathrm{deg}^2]$, gives a 90% acceptance of the γ-rays at SZAs and only 52% acceptance at LZAs. In present analysis we used the orientation cut of $\theta^2 < 0.1\,[\mathrm{deg}^2]$ for LZA observations. Uncertainty in determination of the shower impact distance results in much broader distribution of mean scaled Width for the γ-rays and consequently significantly broader overlap with the cosmic ray events over this parameter. The shape cut $< \tilde{w} > \leq 1.0$ yields the enhancement factor (Q-factor) of 5.3 and 2.0 for the SZAs and LZAs, respectively.

At LZAs the angular size of the images becomes comparable with the pixel size (angular size of photo multiplier in the focal plane) and a small number of pixels is used (about 4) for the image parameterization. In order to improve the analysis at LZAs one can effectively use the fine granularity camera with the pixels of 0.15°. Calculations show that both orientation and shape of Čerenkov light images from air showers at LZAs can be better measured with the camera comprised of smaller pixels.

In order to improve the cosmic ray rejection in observations at LZA we introduced an additional parameter, *mean scaled Length*, $< \tilde{l} >$, defined by analogy with $< \tilde{w} >$. Two parameters, $< \tilde{w} >$ and $< \tilde{l} >$, can be used for calculating a

Mahalanobis distance, MD [4], in two-dimensional space as

$$\mathrm{MD} = ((1- <\tilde{\mathrm{w}}>)^2/\sigma^2_{<\tilde{\mathrm{w}}>} + (1- <\tilde{\mathrm{l}}>)^2/\sigma^2_{<\tilde{\mathrm{l}}>})^{1/2} \tag{1}$$

where $\sigma_{<\tilde{w}>}$ and $\sigma_{<\tilde{l}>}$ are the standard deviations for the corresponding distributions of $<\tilde{w}>$ and $<\tilde{l}>$. We found that the optimum value of the MD cut for LZA is 1.5. Note that this analysis improves the cosmic ray rejection by a factor of 1.7.

The summary of the data is shown in Table 1. Data are shown after applying the orientation cut for the shape analysis by loose mean scaled Width cut of $<\tilde{\mathrm{w}}>< 1.2$ (L. cut), MD cut (MD≤ 1.5) and without image shape cut (Raw).

TABLE 1. Summary of the data taken with the system of 4 IACTs during the observational period from Aug'98 to Dec'98.

	Z.A.	$0° - 25°$	$25° - 40°$	$40° - 50°$	$55° - 65°$
	Time, hrs	7.30	11.34	7.56	5.44
	Raw	592	972	327	143
γ	L. cut	577	670	244	124
	MD cut	450	499	157	101
	Raw	2964	4495	2772	3353
CR	L. cut	536	846	567	658
	MD cut	191	268	151	114
	Raw	7.3	9.7	4.3	1.8
S/N, σ	L. cut	14.2	13.8	6.6	3.3
	MD cut	15.6	15.5	7.3	5.6

The energy of a γ-ray shower is defined by interpolation over the "size" parameter S (total number of photoelectrons in Čerenkov light image) at the fixed impact distance R, as $\mathrm{E} = \mathrm{f_{MC}}(\mathrm{S}, \mathrm{R}, \theta)$, where θ is the zenith angle and $\mathrm{f_{MC}}$ is a function obtained from Monte Carlo simulations. The energy distribution for the ON- and OFF-source events, after the orientation and shape image cuts, were histogrammed over the energy range from 500 GeV to 30 TeV with 10 bins per decade. The γ-ray energy spectrum was obtained by subtracting ON- and OFF-histograms and dividing the resulting energy distribution by the corresponding collection area and the γ-ray acceptance. In the present Crab Nebula analysis we have extended the energy spectrum measurements up to LZAs (65°). The data were processed independently for each of four zenith angle bins: $(0° - 25°), (25° - 40°), (40° - 50°), (50° - 65°)$. The corresponding effective collection areas as well as the cut efficiencies were calculated as a function of the zenith angle. First, we derived the energy spectra for all zenith angle bins independently. Note that the spectra evaluated at different zenith angles are in a good agreement. For the final energy spectrum we joined the different zenith angle bins together

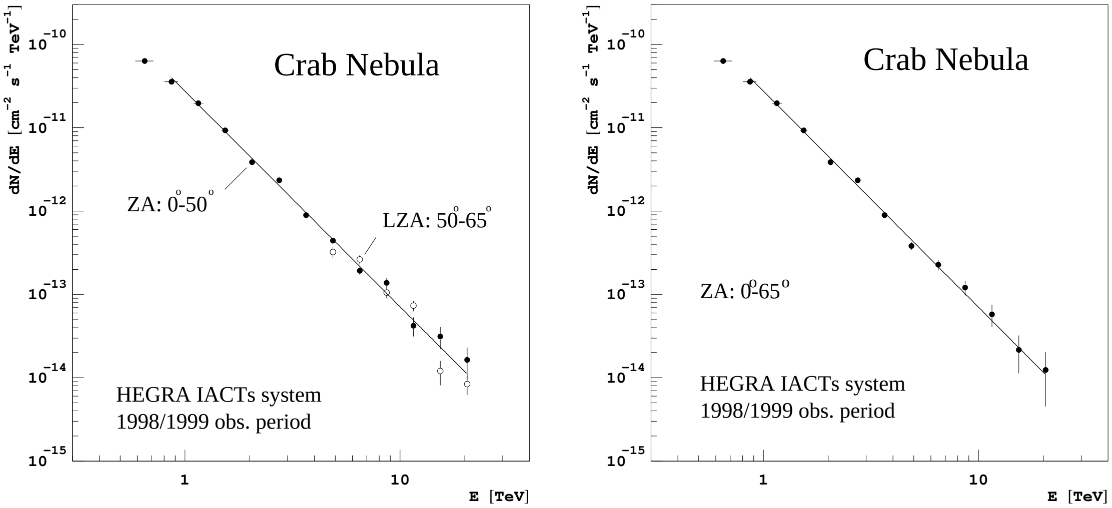

FIGURE 3. The Crab Nebula energy spectrum. The filled circles are for the observations at zenith angles up to 50°, the open circles are for the LZA data (60°).

$$dN^i_\gamma/dE = \sum_{j=1}^{4} w_j (dN^i_\gamma/dE)_j H(E^i - E^j_{th}),$$
$$w_j = t_j/t_0,\ i = 1, n; H = (0, E^i < E^j_{th}; 1, E^i > E^j_{th}) \quad (2)$$

where dN^i_γ/dE, $(dN^i_\gamma)_j/dE$ are the differential energy spectra at energy E^i as measured over all zenith angle range and for the particular zenith angle bin (j), respectively. E_{th} is an estimated energy threshold for the zenith angle bin j. t_j is the observation time for j bin on the zenith angle, and t_0 is the total observation time. $\mathrm{E}^{\mathrm{j}}_{\mathrm{th}}$ is an energy threshold of the γ-rays observed within the zenith angle bin j. The Monte Carlo studies show that for the good energy resolution of 18% this approach does not distort the initial spectrum shape. The collection area for γ-rays rises very quickly in the energy range near the energy threshold of the telescope system, which is 500 GeV, whereas it is almost constant at the energy ≥ 3 TeV. Even slight variations of the trigger threshold could lead to noticeable systematic changes in the predicted spectral behavior in the energy range of $\sim 0.5 - 1$ TeV whereas such effect is negligible for energies above 3 TeV.

Statistics of the γ-rays from the Crab Nebula provides the measurement of the energy spectrum up to a few tens of TeV. However, detection of Čerenkov light images with extremely large amplitudes - several thousands of ph.e. - is complicated by the nonlinearity in the PMT response as well as by saturation in the 8 bit Flash-ADC readout. Such measurements need special treatment [5]. This effect becomes less important in observations at LZAs. Observations at LZAs permit the measurements of the energy spectrum far beyond 10 TeV. The images of the γ-ray air showers observed at LZAs have small *Size* and are not influenced by the saturation effect.

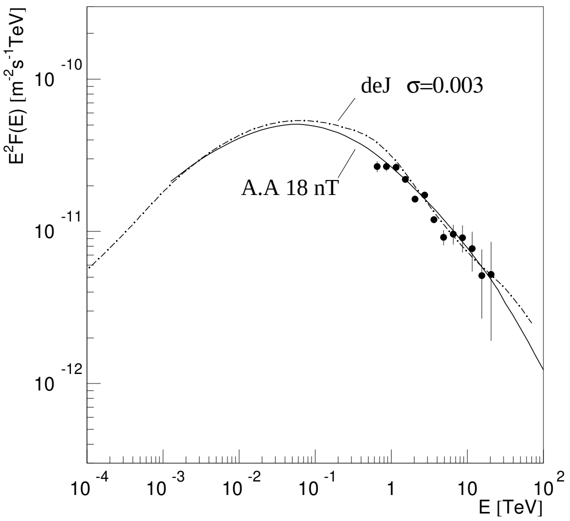

FIGURE 4. The Crab Nebula energy spectrum as measured by HEGRA group. The results of modeling the TeV γ-ray emission from Crab Nebula from [9] (A.A) and [10] (deJ) are shown by solid and dotted-dashed curve, respectively.

RESULTS

We have observed the Crab Nebula extensively in two observational seasons with the HEGRA IACT system. The differential energy spectrum of the Crab Nebula has been derived from the HEGRA data for both observational campaigns using recently developed advanced techniques for the measurements of the spectrum using *stereoscopic data*. The analysis for the different system configurations as well as, for different trigger threshold values give the resulting spectrum

$$\mathrm{dJ}_\gamma/\mathrm{dE} = (2.75 \pm 0.02 \pm 0.5) \cdot 10^{-7} (\frac{\mathrm{E}}{1\,\mathrm{TeV}})^{-2.59 \pm 0.03 \pm 0.05} \mathrm{ph\,m^{-2}\,s^{-1}\,TeV^{-1}} \qquad (3)$$

as measured at zenith angles up to 60°. The statistical and systematic errors are also given.

Based on the Monte Carlo simulations for the γ-ray induced and cosmic ray induced air showers at LZAs, we have developed a specific analysis technique to be used for such data. The Crab Nebula differential energy spectrum derived from small zenith angle data matches quite well the spectrum derived at LZAs. The γ-ray rate measured at energies above 10 TeV in observations at LZAs exceeds the corresponding rate measured at small zenith angles. Our Crab Nebula spectrum is best fitted by a pure power law. To assess the contribution of π^0-produced γ-rays, measurements of the energy spectrum above 30 TeV are necessary.

DISCUSSION

The Crab Nebula has been observed and studied over an exclusively broad photon energy range embracing radio, optical, X-ray bands as well as high energy γ-rays up to hundreds of TeVs. The various theoretical scenarios of photon emission are primarily based on the Synchrotron Compton model [6,7], which combines the synchrotron and inverse Compton (IC) emissions from high-energy electrons, accelerated up to ~ 100 TeV, which interact with magnetic field and seed photons within the nebula [8–10]. The predicted IC spectrum in the TeV energy domain appears to be very sensitive to the model parameters: the value of magnetic field, the nature of seed photons, the maximum energy of electrons, etc. Even IC scenarios of the photon emission are widely believed as most appropriate for the Crab Nebula one can not exclude the possible contribution of the γ-ray fluxes induced by π° decay [9]. The HEGRA data are shown in Figure 4 together with two SSC models of the TeV γ-ray emission [9,10]. One may conclude that IC modeling fits rather well the HEGRA data. According to [9] the estimated magnetic field in Crab Nebula is about 18 nT. To assess the contribution of π^0-produced γ-rays measurements of the Crab Nebula spectrum beyond 20 TeV are needed. The LZA technique could help to perform these future observations.

ACKNOWLEDGMENTS

The support of the German ministry for Research and technology BMBF and of the Spanish Research Council CYCIT is gratefully acknowledged. We thank the Instituto de Astrophysica de Canarias for the use of the site and for supplying excellent working conditions at La Palma. We gratefully acknowledge the technical support staff of the Heidelberg, Kiel, Munich, and Yerevan Institutes.

REFERENCES

1. Aharonian, F., et al., *A & A*, **342**, 69 (1999).
2. Konopelko, A., et al., *J. Phys. G: Nucl. Part. Phys.*, **25**, 1989-2000 (1999).
3. Konopelko, A., et al., *Astoparticle Physics*, **10**, 275-289 (1999).
4. Mahalanobis, H.C., *Proc. Nat. Inst. Sci. India*, **12**, 49 (1963).
5. Hess, M., et al.,*Astroparticle Physics*, **11**, 363-377 (1998).
6. Gould, R.J. *Phys. Rev. Lett.,* **15**, 511 (1965).
7. Kennel, C.F., Coroniti, F.V. *ApJ*, **283**, 694 (1984).
8. De Jager, O.C., Harding, A.K. *ApJ*, **396**, 161 (1992).
9. Atoyan, A.M., Aharonian, F.A. *MNRAS*, **278**, 525 (1996).
10. De Jager, O.C., et al. *ApJ*, **457**, 253, (1996).